Molecular Biology of the Cell
Vol. 21, 3017–3028, September 1, 2010

Chloride Intracellular Channel 4 Is Critical for the Epithelial Morphogenesis of RPE Cells and Retinal Attachment

Jen-Zen Chuang,* Szu-Yi Chou,* and Ching-Hwa Sung*†

*Department of Ophthalmology, and †Department of Cell and Developmental Biology, Weill Medical College of Cornell University, New York, NY 10021

Submitted October 29, 2009; Revised June 1, 2010; Accepted June 29, 2010
Monitoring Editor: Keith E. Mostov

Retinal detachment is a sight-threatening condition. The molecular mechanism underlying the adhesion between the RPE and photoreceptors is poorly understood because the intimate interactions between these two cell types are impossible to model and study in vitro. In this article, we show that chloride intracellular channel 4 (CLIC4) is enriched at apical RPE microvilli, which are interdigitated with the photoreceptor outer segment. We used a novel plasmid-based transfection method to cell-autonomously suppress CLIC4 in RPE in situ. CLIC4 silenced RPE cells exhibited a significant loss of apical microvilli and basal infoldings, reduced retinal adhesion, and epithelial-mesenchymal transition. Ectopically expressing ezrin failed to rescue the morphological changes exerted by CLIC4 silencing. Neural retinas adjacent to the CLIC4-suppressed RPE cells display severe dysplasia. Finally, a high level of aquaporin 1 unexpectedly appeared at the apical surfaces of CLIC4-suppressed RPE cells, together with a concomitant loss of basal surface expression of monocarboxylate transporter MCT3. Our results suggested that CLIC4 plays an important role in RPE-photoreceptor adhesion, perhaps by modulating the activity of cell surface channels/transporters. We propose that these changes may be attributable to subretinal fluid accumulation in our novel retinal detachment animal model.

INTRODUCTION

The retinal pigment epithelium (RPE) is sandwiched between the photoreceptors and choriocapillaries (see Figure 1A). The tight junctions (TJs) formed between the RPE cells prevent passive diffusion of molecules and serve as a blood–retina barrier. Bidirectional transepithelial transport across the RPE critically controls the homeostasis of the subretinal space (SRS) and RPE-photoreceptor adhesion. Unlike most epithelia, which have their apical side face toward the lumen, the apical surfaces of RPE cells are in close contact with the SRS and neural photoreceptors throughout development. On retinal maturation, RPE cells develop fairly long microvilli (MV) extending from their apical surfaces interdigitated into and tightly embracing the light-sensing outer segments (OS) of the photoreceptors. Mature RPE cells also have highly convoluted membranous basal infoldings that directly interact with extracellular matrix of Bruch's basement membrane and the choriocapillaries. The microenvironment of the RPE is important not only for its functions but also its morphogenesis. RPE cells tend to de-differentiate during culture and display only primitive MV and no basal infoldings (Nabi *et al.*, 1993; Dunn *et al.*, 1996). Many RPE proteins are lost in culture or have reversed polarity (Gundersen *et al.*, 1991; Zhao *et al.*, 1997).

The RPE has been identified as the primary site in the etiology of various retinal degenerative diseases, such as age-related macular degeneration (AMD). Furthermore, physical separation between the RPE, or retinal detachment (RD), is a sight-threatening clinical condition seen in macular edema, rhegmatogenous RD, proliferative vitreoretinopathy (PVR), diabetic retinopathy, and central serous chorioretinopathy. Although studies have examined morphological and gene expression changes of the neural retina and RPE after RD (Fisher *et al.*, 2005; Sethi *et al.*, 2005; Zacks *et al.*, 2006; Farjo *et al.*, 2008; Rattner *et al.*, 2008), little is known about the molecular pathogenesis of RD. One major hurdle in studying this question is that the intimate interactions between photoreceptors, RPE, and choroid are extremely difficult to model and study in vitro.

CLIC4 (also called p64H1, huH1, or mtCLIC) belongs to a family of closely related proteins, the chloride intracellular channels (CLIC). CLIC1–CLIC6 share high homology across ~260 amino acids (Ashley, 2003); however, they do not share detectable homology with any other families of chloride channels. CLIC4 generates a Cl^- efflux current upon reconstitution in a synthetic lipid bilayer (Duncan *et al.*, 1997; Littler *et al.*, 2005). However, CLIC4's role as a bona fide channel has been challenged because biochemical studies suggest that CLIC4 is, to a large extent, soluble (Edwards, 1999; Littler *et al.*, 2005). Genetic studies showed that *Caenorhabditis elegans* lacking EXC-4 (the sole CLIC in *C. elegans*) had aberrant luminal expansion in the excretory cells (Berry *et al.*, 2003). These results suggest that CLIC proteins may be involved in steps that are critical for tubulogenesis, such as apical membrane biogenesis, cytoskeletal remodeling, and/or fluid transport (Lubarsky and Krasnow, 2003). CLIC4 has been

This article was published online ahead of print in *MBoC in Press* (http://www.molbiolcell.org/cgi/doi/10.1091/mbc.E09–10–0907) on July 7, 2010.

Address correspondence to: Ching-Hwa Sung (chsung@med.cornell.edu).

detected on various subcellular compartments including MV, cell–cell junctions, centrosomes, mitochondria, large dense core granules, and nuclei among different cell types (Duncan *et al.*, 1997; Chuang *et al.*, 1999; Edwards, 1999; Berryman and Bretscher, 2000; Fernandez-Salas *et al.*, 2002; Berryman and Goldenring, 2003; Suh *et al.*, 2004; Shukla *et al.*, 2009). CLIC4 is susceptible to regulation; for example, CLIC4 was up-regulated in the light-damaged retina (Chen *et al.*, 2004) and in endothelial cells treated with vascular endothelial growth factor (Bohman *et al.*, 2005). Thus, despite the name, CLIC4 may have a variety of discrete cellular functions in various physiological contexts.

In this report, we describe a tissue-specific, effective, and versatile approach to manipulate gene expression in rodent RPE in situ. Using this method, we investigated the function of CLIC4. We found that CLIC4 is highly enriched in the apical RPE MV, and plays a cell-autonomous role in the epithelial morphogenesis of RPE and in the interaction between RPE and neural photoreceptors. Silencing CLIC4 in RPE is sufficient to induce RD and retinal atrophy. The mechanistic studies show CLIC4 silencing–mediated phenotypes are not simply accountable by the loss of MV processes.

MATERIALS AND METHODS

Reagents

Anti-CLIC4 rabbit antibody (Chuang *et al.*, 1999), Anti-ezrin mouse Ab (Abcam, Cambridge, MA), rhodopsin mAb (clone B-6-30; gift of Paul Hargrave), ZO-1 (Millipore, Billerica, MA), anti-GFAP mouse antibody (Sigma, St. Louis, MO), anti-AQP-1 rabbit antibody (gift of W. Daniel Stamer; Stamer *et al.*, 2003), anti-NKCC1 rabbit antibody (gift of Jim Turner; Moore-Hoon and Turner, 1998), anti-MCT1 and anti-MCT3 rabbit antibodies (gifts of Nancy Philp; Philp *et al.*, 2003), Na/K-ATPase (DHSB), and Alexa594- or fluorescein-conjugated phalloidin (Invitrogen, Carlsbad, CA). Various Alexa-dye–conjugated secondary antibodies (Invitrogen), Cy5-conjugated secondary antibodies (Jackson ImmunoResearch, West Grove, PA), and goat anti-rabbit IgG conjugated to 1-nm gold particles (AuroProbe One, Amersham Pharmacia Biotech, Piscataway, NJ) were also used. The CLIC4-sh and ezrin-sh plasmids were constructed in pBS/U6 vector (gift of Yang Shi) as described previously (Xia *et al.*, 2003) using 5′-GGGCTCTTGAAAACGCTGCAG-3′ and 5′-GGGTCCTATGCCGTTCAGGCC-3′ oligos as targeting sequences, respectively. The scrambled control-sh plasmid was purchased from Ambion (Austin, TX). The DNA fragments containing either U6-CLIC4-sh, U6-ezrin-sh, or U6-control-sh were then inserted into pCAG-HcRed or pCAG-mGFP vector (gift of Connie Cepko) in which the HcRed cDNA or mGFP were under the control of chicken-β-actin (CAG) promoter. To generate CLIC4-sh/vsvg-ezrin plasmid for the rescue experiments, human vsvg-ezrin was excised from pCB6-Eztag (Algrain *et al.*, 1993; gift of Dr. Monique Arpin) and inserted into CLIC4-sh/mGFP between CAG promoter and IRES. Similar strategies were also used to generate to a plasmid encoding ezrin-sh, vsvg-ezrin, and monomeric green fluorescent protein (mGFP), and a plasmid encoding vsvg-ezrin and mGFP. Dog CLIC4 cDNA was generated by RT-PCR of RNA isolated from Madin-Darby canine kidney epithelial cells. RPE-J cells are cultured and transfected as described (Finnemann *et al.*, 1997).

In Vivo RPE Transfection and Analysis

For in vivo RPE transfection, 1 μl of plasmid (3 μg/μl in Tris-EDTA buffer) was injected into the SRS of neonatal (PN1-PN3) Sprague-Dawley rats, followed by electroporation using a pair of tweezer-type electrodes (BTX, Hawthorne, NY), which were placed across the eyes so that the cathode faced to cornea and the anode faced the sclera. Five 100-V pulses were given with 50-ms duration and a 950-ms resting interval. Animals were housed in a 12-h light-dark cycle and harvested at postnatal day 21. At least three animals were examined for each experiment. All methods involving live animals were approved by the Weill Medical College of Cornell University Institutional Animal Care and Use Committee.

Light Microscopic and EM Analyses of Retina

For both immunolocalization and ultrastructural analyses, anesthetized animals were transcardially perfused through the ascending aorta with 1) 10 ml of heparin saline (1000 U/ml), 2) 20 ml of 4% PFA/3.75% acrolein (Polysciences, Warrington, PA) in 0.1 M phosphate buffer (pH 7.4), and 3) 60 ml of 4% PFA in 0.1 M phosphate buffer. The eyes were subsequently enucleated and then prepared for eye cups. The eye cups were further fixed in 4% PFA/0.1% glutaraldehyde in 0.15 M cacodylate buffer (pH 7.4) overnight before the agarose embedding and vibratome sectioning. Immunolabeling was carried out using free-floating methods previously described (Chuang *et al.*, 2001). All immunolabeled sections were examined with a Leica TCS SP2 microscope (Nussloch, Germany) with a HCX PL APO 63×/1.4 NA oil CS Blue objective using Leica Confocal Software. For ultrastructural analysis, retinal sections were permeabilized by the freeze-thaw method (Chan *et al.*, 1990), immunolabeled, and postfixed with 2% glutaraldehyde for 10 min after the secondary Ab incubation, as described (Chuang *et al.*, 2001). The immunolabeled sections were then processed for silver-enhancement, OsO_4 fixation, and dehydration. Finally, the sections were then flat-embedded in Epon, and further cut into 70-nm-thick ultrathin sections followed by an examination on a Philips CM10 electron microscope (Mahwah, NJ). Negative controls were treated identically and in parallel except that primary Abs were omitted. In some experiments, conventional electron microscopy (EM) was carried out using the same procedures except that the immunolabeling steps were omitted.

RESULTS

CLIC4 Is Enriched in the Apical MV of RPE Cells

To examine CLIC4 localization, we used an affinity-purified anti-CLIC4 antibody that did not cross-react with other CLIC proteins (Chuang *et al.*, 1999). At postnatal day (PN) 1, MV processes and photoreceptor OS are not yet developed, and prominent CLIC4 immunofluorescence was detected at the apical surface of RPE cells (Figure 1B). In adult RPE, CLIC4 was rich in the long, extended MV processes that were deeply interdigitated into rhodopsin-labeled photoreceptor OS (Figure 1, C and D), even though cytoplasmic CLIC4 signal was also observed.

Ultrastructural examination confirmed that CLIC4-derived silver-enhanced immunogold particles were enriched on the long, slender MV, and these particles were in close proximity to the plasma membranes (Figure 1, E and F). Pseudopodial processes that surrounded the disk undergoing shedding were also often labeled by CLIC4 immunogolds (Figure 1G). Finally, CLIC4 immunogolds were also associated along with the TJs (arrows in Figure 1H). Preincubation of antibodies with antigen almost completely abolished these signals (data not shown).

In Situ Suppression of CLIC4 Decreases the Attachment between RPE and OS

To study CLIC4's function in the RPE in situ, we modified an in vivo retinal transfection method (Matsuda and Cepko, 2004) to perform RPE-specific gene delivery. Plasmid under the regulation of chicken β-actin (CAG) promoter was injected into the subretina of neonatal rodent eyes (Figure 2A; see *Materials and Methods*), followed by electroporation using tweezer electrodes across the eyes, with the cathode facing cornea and the anode facing the sclera (Figure 2B). Observation of the fluorescence derived from the transfected plasmid encoding either red fluorescent protein HcRed (Figure 2D) or GFP (Figure 2E) suggested that this gene transduction method was highly efficient and specifically restricted to the RPE (Figure 2, D and E). No fluorescent signal was detected in neighboring photoreceptors or choroids (Figure 2E), and the protein expression persisted for at least 6 wk after transfection (data not shown). The animals used for the studies described in this article were 3 wk old. At this time point, both the retina and RPE are fully developed.

To study CLIC4 using a loss-of-function approach, we generated a plasmid-based short hairpin RNA (sh) specifically against rat CLIC4. In addition, cDNA encoding either HcRed or membrane-bound GFP was also added to the same vector (i.e., CLIC4-sh/HcRed or CLIC4-sh/mGFP; Figure 3A) so that the targeted cells can be unambiguously identified. The mGFP reporter was used to facilitate the visualization of RPE plasma membranes under light microscopy. The silencing effect was first validated in transiently

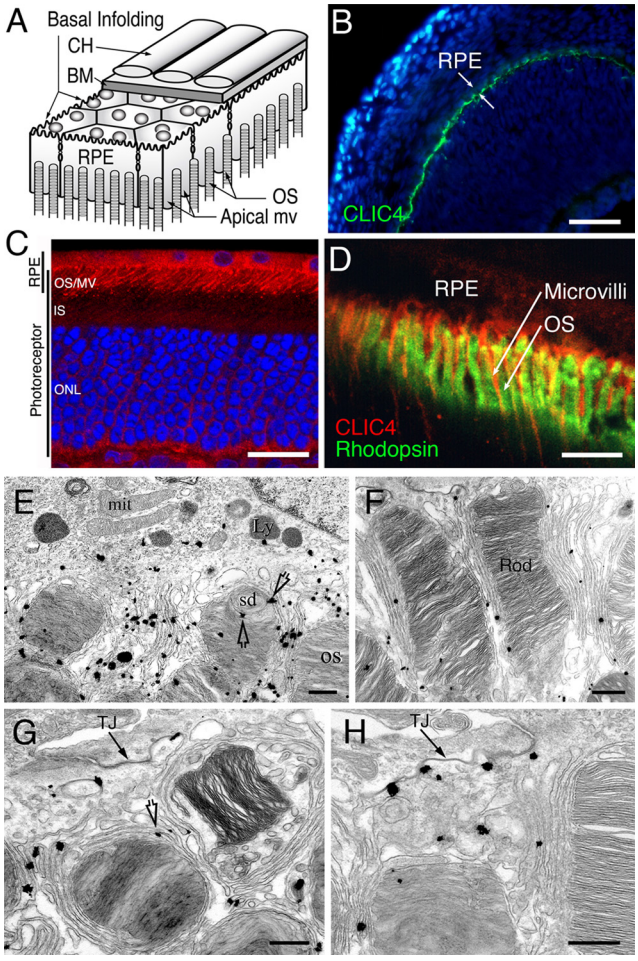

Figure 1. Schematic diagram of RPE in situ and the CLCI4 distribution in RPE. (A) A three-dimensional drawing showing the relationship between photoreceptor OS, RPE, Bruchs basement membrane (BM), and choriocapillaries (CH). (B–D) Confocal analysis of PN1 (B) and adult (C and D) rat retinas that were immunolabeled for CLIC4 (green in B; red in C and D). Rhodopsin (green) was also colabled in D. Blue, DAPI-stained nuclei. (E–H) Electron micrographs of the RPE-photoreceptor interphase. Arrows in G and H point to the CLIC4 immunogolds affiliated with the TJ. Ly, lysosome; Sd, disk undergoing shedding. Bars, (B) 50 μm; (C) 20 μm; (D) 10 μm; (E–H) 0.5 μm.

transfected RPE-J cell line by immunoblotting assay (Figure 3B). RPE tissues transfected with CLIC4-sh/HcRed or CLIC4-sh/mGFP were examined by confocal microscopy in either whole mount sheets (Supplemental Figure 1; Figures 2D, and 3C) or transversely sectioned retinal slices (Figure 3D). CLIC4-sh/HcRed and CLIC4-sh/mGFP produced a similar knockdown effect; greatly reduced endogenous CLIC4 was seen in transfected cells compared with the neighboring nontransfected cells (Supplementary Figure 1; Figures 3C and 3E). These two targeting constructs were therefore used interchangeably in the subsequent experiments.

The mGFP signal derived from the control-sh marked both apical and basal plasma membranes of RPE (Figure 3D, bottom). The apical signal was closely associated with the ezrin-labeled MV, which were morphologically indistinguishable from those of neighboring, nontransfected cells. By contrast, the apical MV of almost all CLIC4-sh–targeted cells had an abnormally short and "compact" appearance (Figure 3D, top; 98.6 ± 0.9%; n = 129 cells in three animals).

We subsequently performed a rescue experiment to rule out that the morphological change of the MV seen in CLIC4-sh–transfected cells was an off-target effect. To this end, a plasmid encoding dog CLIC4 cDNA was cotransfected with CLIC4-sh/mGFP; the transfected cells were identified based on the GFP signal and the CLIC4 immunolabeling. Figure 3E shows a representative retinal section containing four RPE cells. Cell 1 is a GFP-negative, nontransfected cells that had basal level of CLIC4. Cell 4 is a cell singly transfected with CLIC4-sh/mGFP that had reduced CLIC4 level and shortened MV. Cells 2 and 3 are cells cotransfected with both CLIC4-sh/mGFP and CLIC4; the CLIC4 levels of these cells were restored to match (or slightly higher than) the endogenous CLIC4 level (i.e., cell 1). The MVs of cells 2 and 3 were indistinguishable from that of cell 1.

To determine if the altered apical appearance of CLIC4-suppressed RPE cells functionally reduced their interaction with photoreceptor OS, we performed en face examination of RPE sheets that were peeled off from the retinas (Figure 3C), and counted the numbers of rhodopsin-labeled OS tips that remained adhered to the RPE surfaces. About 60 ± 11 OS tips were found in single nontransfected cells; this number is within the range of the numbers of photoreceptors that are enwrapped by the RPE MV. In contrast, significantly fewer OS tips were attached to the apical surfaces of CLIC4-sh/mGFP–transfected RPE cells (12 ± 4 per cell; Figure 3C), indicating reduced retina-RPE adhesion.

Ectopically Expressed Ezrin Cannot Rescue Phenotypes Mediated by CLIC4 Suppression

Ezrin has been shown to play a key role in the MV genesis of various epithelial cell types including RPE (Bretscher, 1989; Bonilha *et al.*, 1999; Tsukita and Yonemura, 1999; Yonemura and Tsukita, 1999; Bonilha *et al.*, 2006). The RPE MV of 10-d-old ezrin knockout mice are shorter than those of the age-control mice (note that these animals die before the retina matures; Bonilha *et al.*, 2006). To examine the adult RPE cells in which ezrin was suppressed, we transfected (rat-specific) ezrin-sh/GFP plasmid in rat eyes. Almost 100% of the targeted RPE cells had much reduced ezrin signals and displayed shortened MV processes (Figure 4A).

We subsequently performed the rescue experiment to validate the ezrin-sh–mediated phenotype; a cDNA encoding vesicular stomatitis virus glycoprotein G (vsvg)-tagged human ezrin (herein referred to as vsvg-ezrin) was used for this purpose. To improve the codelivery efficiency, a single rescue plasmid containing ezrin-sh, vsvg-ezrin, and mGFP was generated and used for transfection (Figure 4B). The mGFP$^+$-transfected cells typically had a slight increase in ezrin labeling (arrowhead in Figure 4C); the vast majority of these cells (~98%) had a normal MV appearance (Figure 4C, arrow). These results, taken together, arguing that the result obtained from the in vivo RPE transfection mirrored that obtained from the conventional transgenic mouse approach.

We then asked whether forced expression of ezrin could restore the MV morphogenesis in CLIC4-silenced RPE cells. To this end, a plasmid encoding CLIC4-sh, vsvg-tagged ezrin, and mGFP (Figure 4D) was transfected into RPE cells. As an example shown in Figure 4E, a mGFP$^+$-transfected cell had an increased level of ezrin, but its CLIC4 level remained lower compared with the nontransfected cells. This showed that excess ezrin was unable to restore the level of CLIC4. Ectopically expressed ezrin was predominantly distributed in the mGFP$^+$ apical surfaces. En face confocal examination of ectopically expressed ezrin (using vsvg an-

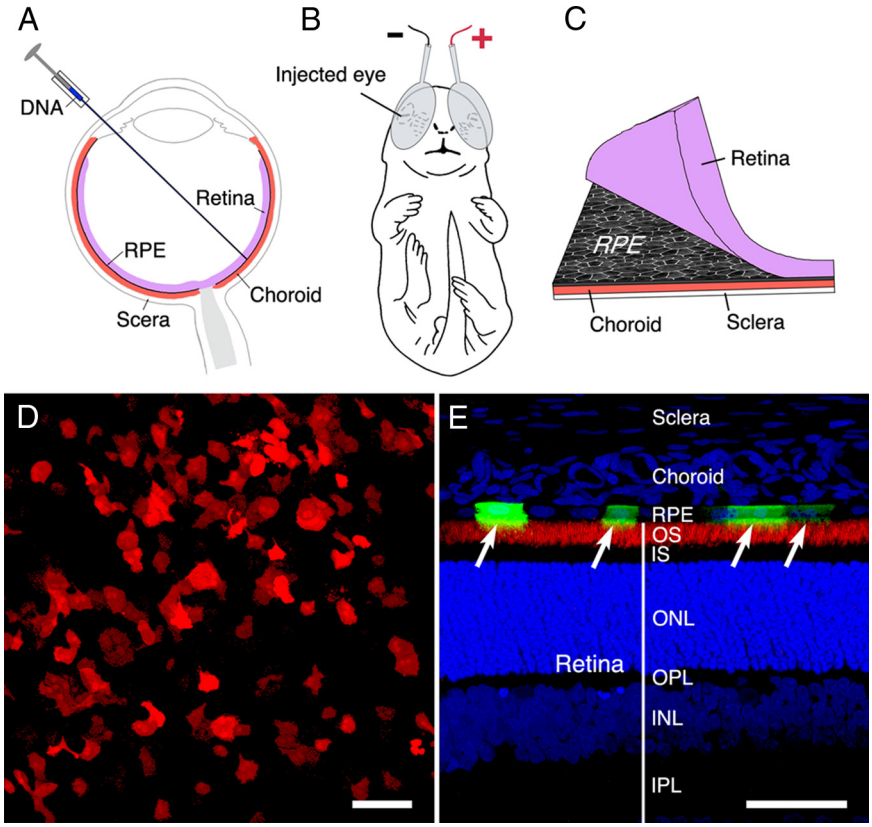

Figure 2. Plasmid-based RPE transfection in situ. (A and B) Schematic drawing of the subretinal injection (A) and electroporation procedures (B) of neonatal animals. (C) Schematic drawing of the preparation of retina-free whole-mount RPE sheets. (D) En face view of HcRed-transfected RPE cells. (E) Retinal section containing mGFP-transfected RPE cells (arrows); OS were labeled with rhodopsin (red). Blue, DAPI-stained nuclei; IS, inner segment; ONL, outer nuclear layer; OPL, outer plexiform layer; INL, inner nuclear layer. Bar, (D) 100 μm; (E) 50 μm.

tibody) and mGFP showed that these apical surfaces resembled membrane ruffles, rather than MVs (Figure 4F). These ruffled structures were not interdigitated into the adjacent photoreceptor OS, and the expanded SRSs between the RPE and MV remained (arrow in Figure 4E; 96.5 ± 1.1%; n = 740 cells in three animals).

The results discussed above suggested that overexpressed ezrin failed to rescue the phenotypes of CLIC4 silencing. This is somewhat unexpected because Bonilha *et al.*, (1999) showed that ezrin overexpression increased the MV length of the RPE cells in culture (i.e., RPE-J cell line). RPE-J cells have almost no microvilli and they develop 1-μm-long microvilli upon stable expression of vsvg-ezrin (Bonilha *et al.*, 1999). To directly test whether excess ezrin alone is sufficient to alter the RPE MV appearance in situ, we examined the cells transfected with a plasmid that encoded both vsvg ezrin and mGFP (Figure 4G). The majority of these cells displayed typical MV (76%; n = 46 cells in three animals; Figure 4H), and ~24% of them had membrane ruffles (data not shown).

CLIC4 Silencing Triggers Atrophy in Both RPE and Neural Retina

Signs of major tissue remodeling and atrophy of both RPE and neuronal retinas were displayed in the eyes with RPE targeted with CLIC4-sh/HcRed (Figure 5, A, B, and D). Most interestingly, many of these phenotypes were similar to those seen in an acutely induced RD animal model (Steinberg, 1986; Fisher *et al.*, 2005). For example, the photoreceptor OS underneath CLIC4-sh/HcRed-targeted RPE cells were often overgrown and bent (Figure 5D). The outer nuclear layers were highly deformed, with photoreceptors undergoing delamination, overproliferation, and forming rosettes (Figures 5B, bottom, and 5D). Disorganization of the inner retina was also often observed (Figure 5B). All these changes produce an uneven retinal thickness from region to region. Like other examples of injured photoreceptors and stressed retina (Bringmann and Reichenbach, 2001), the expression of glial fibrillary acidic protein (GFAP) in the reactive Muller cells was dramatically increased in these retinas (Figure 5C). Furthermore, a series of confocal microscopic examinations showed that many CLIC4-sh/HcRed–transfected RPE cells were detached from their underlying basement membrane and became migratory; the HcRed+ cells were found in the "torn" SRS (arrow in Figure 5D). No similar phenomenon was associated with the eyes transfected with control-sh/HcRed (Figure 5C, inset) or control-sh/mGFP (see Figure 3D, bottom).

CLIC4 Is Essential for the Epithelial Morphogenesis of RPE

The increased motility seen in the CLIC4-silenced RPE cells and the appearance of CLIC4 signal at the TJ prompted us to examine the structural integrity of the TJ in these cells using ZO-1 immunolabeling. The nontransfected cells or cells targeted with control-sh/HcRed had a continuous circumferential band pattern of ZO-1 labeling, whereas CLIC4-sh/HcRed–targeted RPE cells had broken and displaced ZO-1 labeling (arrows in Figure 6A).

We examined the F-actin microfilament organization of the CLIC4-suppressed RPE cells using fluorescein-conjugated phalloidin. En face confocal analysis of RPE sheets showed abundant F-actin distributed in the cell cortex, forming circumferential rings (Figure 6B). The CLIC4-sh/HcRed–transfected cells exhibited prominent stress fiber-like structures (arrows, Figure 6B), that were absent in neighboring

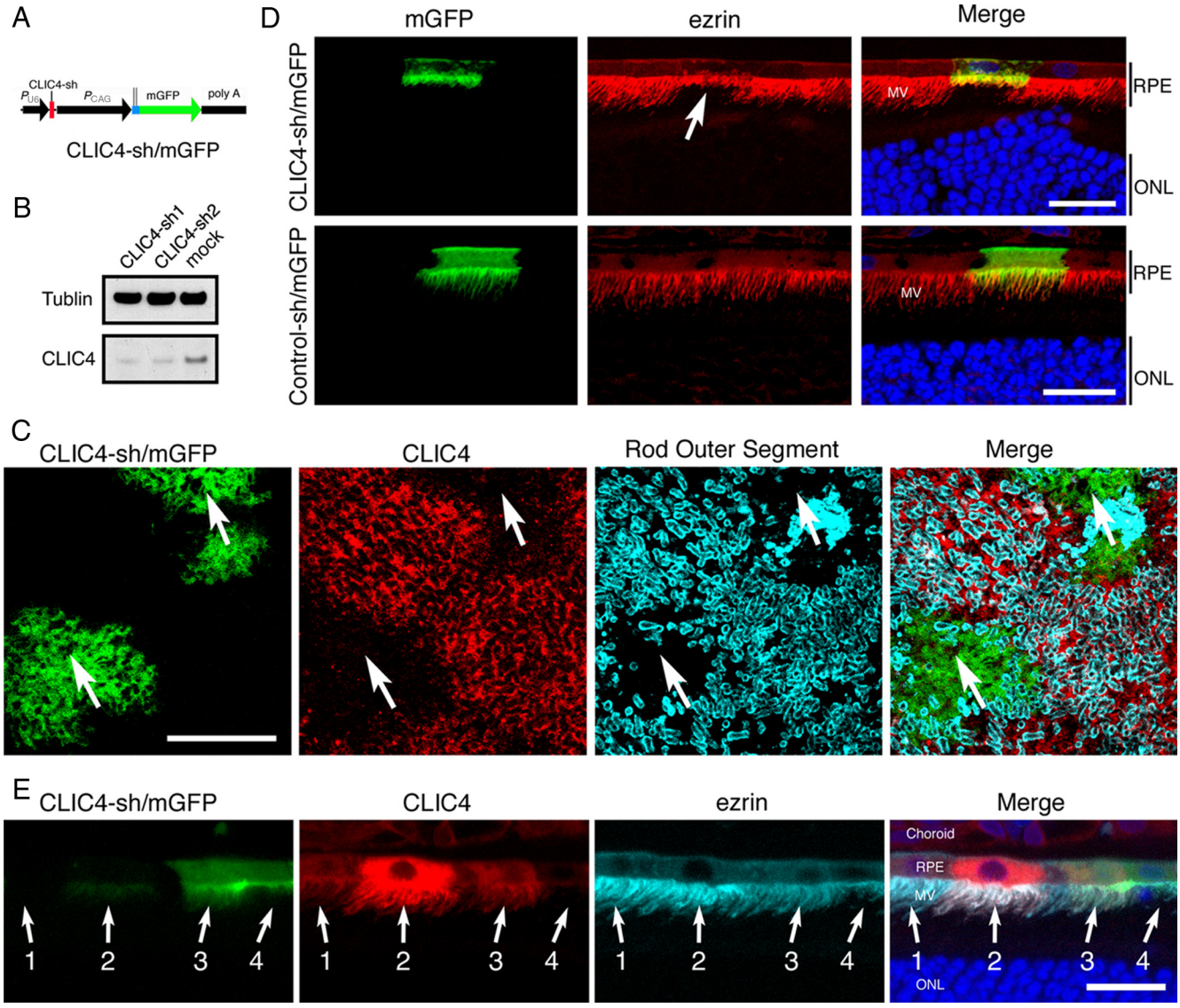

Figure 3. CLIC4 silencing in RPE in situ. (A) Diagram of CLIC4-sh/mGFP plasmid. (B) Immunoblotting of CLIC4-sh–transfected RPE-J cell lysates. (C) En face confocal images of a flat whole-mount RPE sheet transfected with CLIC4/mGFP plasmid and immunolabeled for CLIC4 (red) and rhodospin (cyan). Arrows point to the GFP-transfected cells. (D) Confocal images of retinal sections in which the RPE cells have been transfected with either CLIC4-sh/mGFP or control-sh/mGFP and immunolabeled for ezrin (red). (E) Confocal images of retinal sections in which the RPE cells have been cotransfected with CLIC4-sh/mGFP and dog CLIC4 and immunolabeled for CLIC4 (red) and ezrin (cyan). Arrows point to four cells: a nontransfected cell (1), two double-transfected cells (2 and 3), and a cell singly transfected with CLIC4-sh/mGFP (4). Bars, 20 μm.

nontransfected cells. In addition, F-actin was also rich in basal infoldings at the basal focal plane of control RPE cells (Figure 6B, bottom). In stark contrast, the basal F-actin labeling disappeared in CLIC4-sh/HcRed–targeted cells, indicating their loss of basal infoldings (Figure 6B, asterisks). The changes seen in CLIC4-suppressed RPE cells—TJ dissolution (see more in Figure 7E), monolayer disintegration, loss of specialized epithelial membranous structures, gain of fibroblast features—suggest that these cells undergo an epithelial-mesenchymal-transition.

Ultrastructural Examination of the Morphological Changes in RPE with Reduced CLIC4

We further examined the morphological alterations caused by CLIC4 silencing in RPE at the ultrastructural level using preembedding EM. In these experiments, CLIC4-sh/mGFP–transfected RPE cells were identified by the presence of GFP-labeled immunogolds, and these cells can be directly compared with adjacent nontransfected GFP-negative cells in a side-by-side manner. As shown in the represented electron micrographs, the long MV (~23-μm_{ave} length) of nontransfected cells were longitudinally arrayed and interdigitated into the photoreceptor OS (marked as $shRNA^-$ in Figure 7, A and B). In sharp contrast, the MV of CLIC4-sh–targeted RPE cells (marked as $shRNA^+$ in Figure 7A) were very short and ~2.3-μm_{ave} length (Figure 7C). These MV processes were often oriented away from the OS, leaving an expanse of space between the remaining MV processes and the OS (arrows in 7C). The OS lying near the CLIC4-sh–transfected RPE cells was often turned sideways, evi-

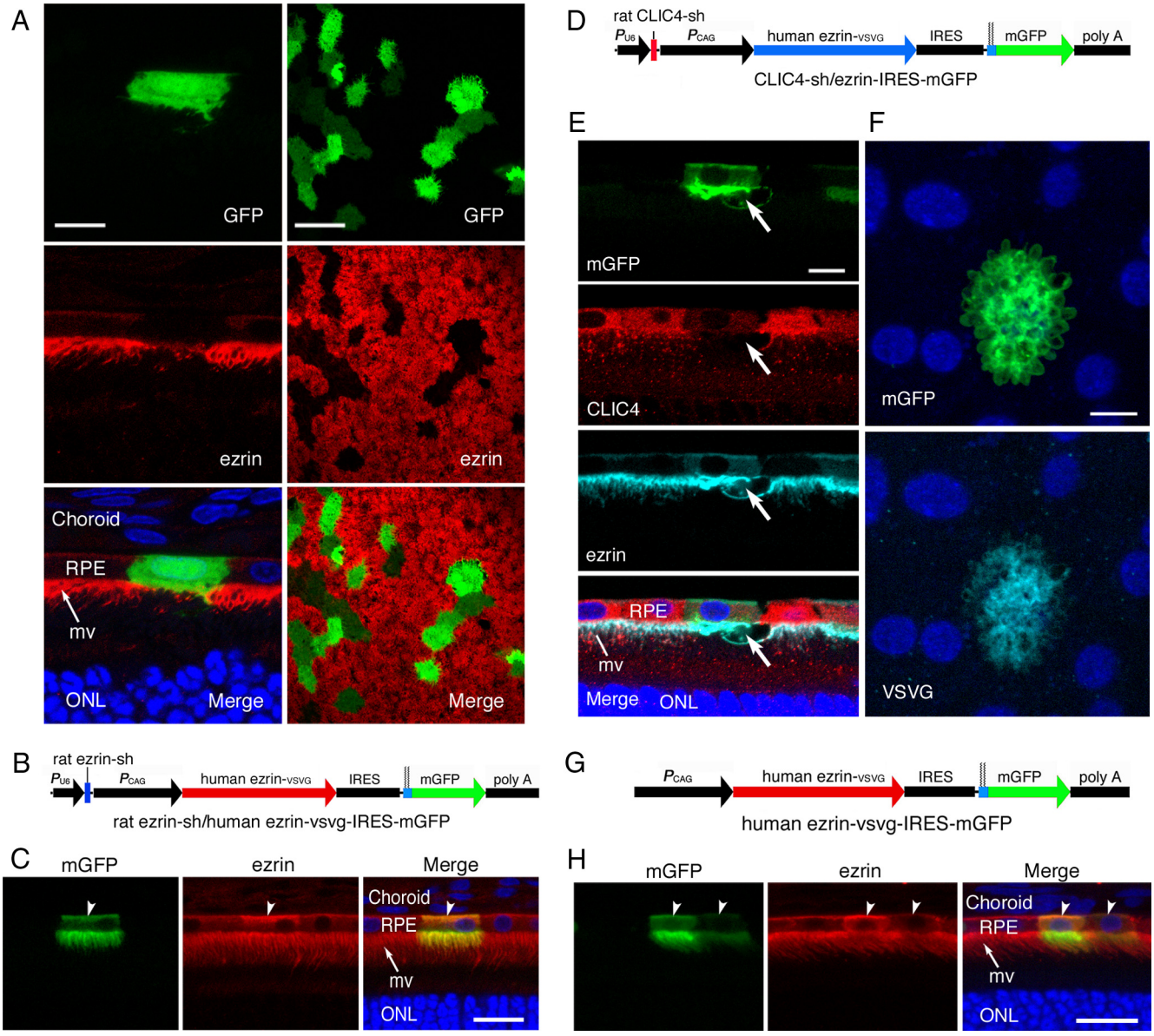

Figure 4. Ezrin silencing in RPE in situ. (A) Confocal images of transverse retinal section (left) and whole-mount RPE sheet (right) containing ezrin-sh/GFP plasmid-transfected cells immunolabeled for ezrin (red). (B) Diagram of the plasmid that encodes ezrin-sh, vsvg-ezrin, and mGFP. (C) Confocal images of transverse retinal section containing ezrin-sh/vsvg-ezrin/mGFP–transfected cells immunolabeled for ezrin (red). Arrowheads pointed to a GFP^+ cell displaying modestly increased ezrin and normal MV appearance. (D) Diagram of the plasmid that encodes CLIC4-sh, vsvg-ezrin, and mGFP. (E, F) Transverse retinal sections (E) or whole-mount RPE sheet (F) containing RPE cells transfected with the CLIC4-sh/vsvg-ezrin/mGFP plasmid and followed by immunostaining for CLIC4 (red) and ezrin (cyan; E), or vsvg-epitope (cyan; F). (G) Diagram of the plasmid encodes vsvg-ezrin and mGFP. (H) Confocal images of retinal section containing ezrin overexpressed cells that immunolabeled for ezrin (red). Two GFP^+ cells show increased ezrin immunolabeling that exhibited MV with normal appearance (arrowheads). Bar, (A, left; E and F) 10 μm; (C and H) 20 μm; (A, right) 50 μm.

denced by their tangential sectioned planes relative to the neighboring OSs of nontransfected RPE cells. These images confirmed and explained the reduced intimacy between RPE and photoreceptors that we observed at the light microscopic level. Finally, it is of interest to note that CLIC4-suppressed cells exhibited "cytoplasmic inclusions" that contained several MV process-like membranous stacks, which were not seen in the control cells (arrows, Figure 7D).

The basal infoldings are a prominent feature of RPE cells; these convoluted membrane folds occupied a ~1.5-μm-thick space at the basal part of the cell (open arrows in Figure 8, A and B). In stark contrast, basal infoldings were almost completely absent in CLIC4-sh–transfected cells (Figure 8, A and C). Finally, typical TJs were difficult to find in CLIC4-sh–transfected cells (arrows in Figure 7E vs. Figure 1, G and H).

Consistent with our light microscopic analysis (Figure 5D), CLIC4-sh–transfected RPE cells migrating into the SRS were also readily seen in our surveys (Supplemental Figure 2). Taken together, our ultrastructural investigation provided a confirmation of all the CLIC4-silencing induced phenotypes based on the immunocytochemistry and confocal microscopy-based assays, reiterating the role of CLIC4 in

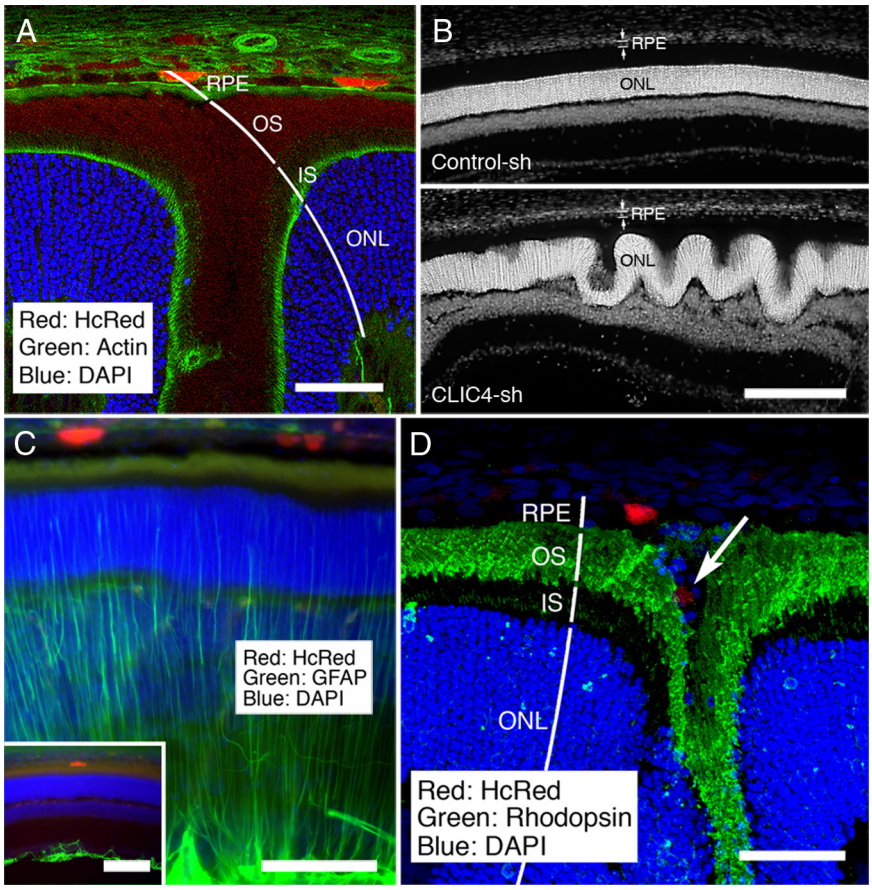

Figure 5. CLIC4 suppression in RPE induced RD and retinal atrophy. (A–D) Representative confocal images reveal the disorganization and dysplasia of the retinas adjacent to the CLIC4-sh/HcRed–transfected RPE cells. Immunolabeling was carried out by indicated antibodies (A, C, and D) or DAPI (B). GFAP labeling of the retina containing control/HcRed–transfected RPE cells was shown in the inset of C. Arrow in D points to a HcRed$^+$ RPE cell that has migrated into the abnormally expanded SRS. Bars, (A and D) 50 μm; (B) 200 μm; (C) 100 μm.

the morphogenesis of both membranous and junctional structures of RPE in situ.

Channel and Transporter Expression Are Altered in CLIC4 Suppressed RPE Cells

The increased SRS underneath the RPE cells with CLIC4-suppressed was an indication of imbalanced water homeostasis and fluid accumulation. We examined the expression patterns of several proteins thought to be involved, directly or indirectly, in fluid transport in RPE cells: Na^+-K^+-$2Cl^-$ cotransporter (NKCC1; Edelman and Miller, 1991), NaK-ATPase, proton-coupled monocarboxylate transporter (MCT; Hamann *et al.*, 2003), and aquportin (AQP; Nielsen *et al.*, 1993; Oshio *et al.*, 2005). Our results showed that the apical MV localizations of NKCC1 and Na/K-ATPase were not significantly affected by the loss of CLIC4 (data not shown). MCT3, which was typically expressed in the basal RPE surface (Philp *et al.*, 1998), was specifically absent in CLIC4-sh/mGFP (Figure 9A, middle) and CLIC4-sh/vsvg-ezrin/mGFP transfected RPE cells (Figure 9A, bottom). By contrast, the expression of MCT3 was not affected in control-sh (Figure 9A, top) as well as ezrin-sh/GFP–transfected

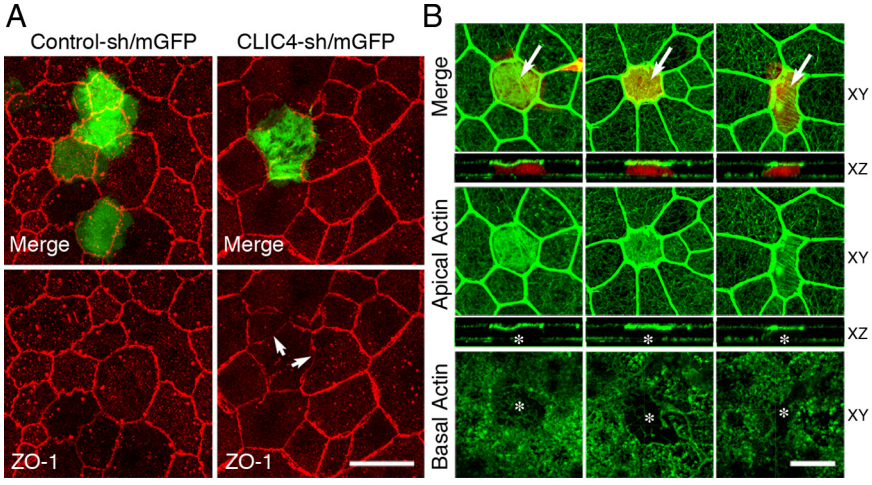

Figure 6. CLIC4 suppression affects the cell–cell junctional and microfilament organizations of RPE cells (A) RPE sheets containing CLIC4-sh/mGFP or control-sh/mGFP–transfected cells immunolabeled with anti-ZO-1 antibody. Arrows point to the displaced ZO-1 labeling in a CLIC4-sh–targeted cell. (B) Images of confocal en face scanning reveal the F-actin labeling (green) in three CLIC4-sh/HcRed–targeted cells. Images taken at both subapical (middle) and basal (bottom) sides of the cells are shown. Arrows point to the stress fiber-like meshwork displayed in the HcRed$^+$-targeted RPE cells. Asterisks point to the CLIC4-sh/HcRed–targeted cells that have lost actin-rich basal infoldings. Bars, 20 μm.

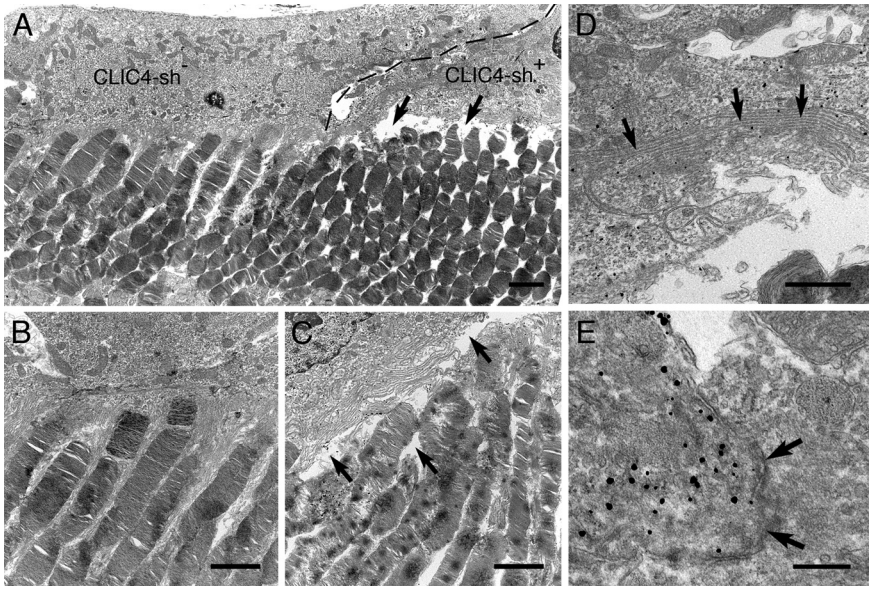

Figure 7. Ultrastructural examination of CLIC4-silenced RPE cells in situ. Electron micrographs of retinal sections containing RPE cells transfected with CLIC4-sh/mGFP, identified by the positive labeling of GFP-immunogold (marked as CLIC4-sh$^+$), and their adjacent nontransfected RPE cells (marked as CLIC4-sh$^-$). Dotted lines marked the cell borders. Low-power (A) and high-power images of apical sides of nontransfected (B) and transfected (C) cells are shown. (D) MV-like "noodles" accumulated in the cytoplasm of a CLIC4-sh–transfected cell are shown (arrows). (E) A representative image shows that the TJ in a CLIC4-sh–transfected cell is not typical. Bars, (A–C) 2 μm; (D) 1 μm; (E) 0.3 μm.

cells (Supplemental Figure 3). Finally, the apical protein MCT1 (Philp *et al.*, 1998) was, however, unaffected in CLIC4-suppressed cells (data not shown).

Previous immunohistochemistry studies have shown that there are no AQP expressed in rodent RPE cells in situ (Nielsen *et al.*, 1993; Hamann *et al.*, 1998; Stamer *et al.*, 2003; Verkman *et al.*, 2008). However, AQP1 has been detected in human RPE in cultures (Ruiz and Bok, 1996; Stamer *et al.*, 2003) and in situ, using a highly sensitive surface biotinylation method (Stamer *et al.*, 2003). In our hands, AQP1 is detected in photoreceptor OS, as reported (Iandiev *et al.*, 2005), but not in RPE cells of control animals (Figure 9B, top, arrows). By contrast, strikingly intense AQP1 signal was specifically detected in the apical surface of the vast majority of CLIC4-suppressed RPE cells (arrows in Figure 9B, middle; Supplemental Figure 4, bottom; 95.4 ± 2.0%, n = 494 cells in four different animals). The AQP1 expression in the photoreceptor OS in these animals was not detectably affected. The activation of AQP1 in CLIC4-suppressed RPE cells was rather specific. No increase of AQP1 signal was detected in ezrin-sh/RPE cells (Supplemental Figure 4, top and middle), and ezrin overexpression did not prevent the up-regulation of AQP1 in CLIC4-suppressed cells (Figure 9B, bottom). Finally, AQP2 was not expressed in either control or CLIC4-suppressed RPE cells (data not shown). These re-

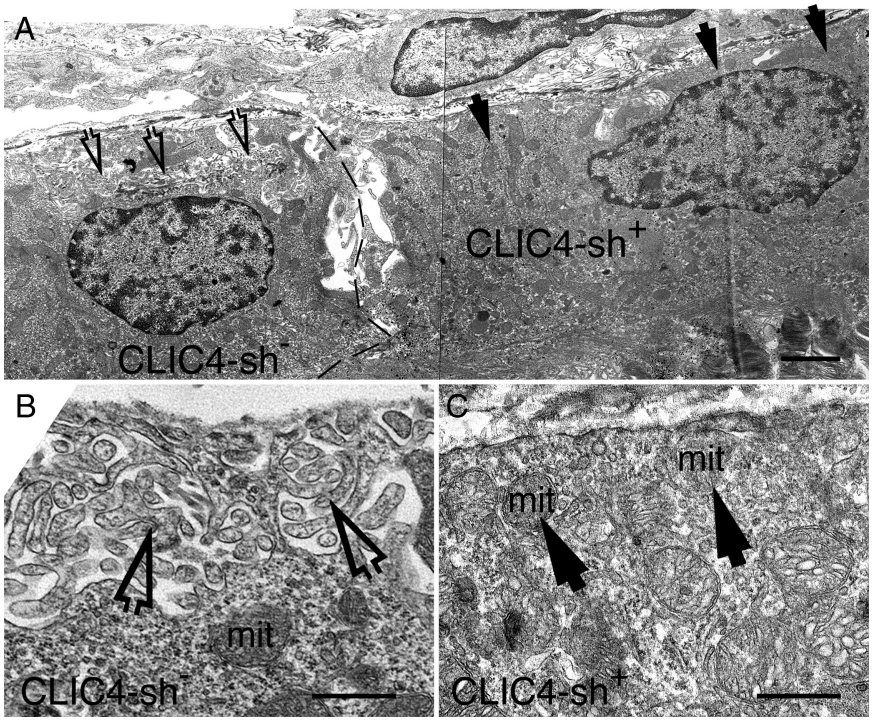

Figure 8. Ultrastructural examination of the basal aspect of CLIC4-silenced RPE cells in situ. Low-power (A) and high-power images of basal sides of nontransfected (B; CLIC4-sh$^-$) and transfected (C; CLIC4-sh$^+$) cells are shown. Open arrows point to the basal infoldings in a nontransfected cell. Black arrows point to the basal side of a CLIC4-sh–transfected cell completely lacks basal infoldings; this region was filled with cytoplasm containing abundant mitochondria (mit) instead. Bars, (A) 2 μm; (B and C) 0.5 μm.

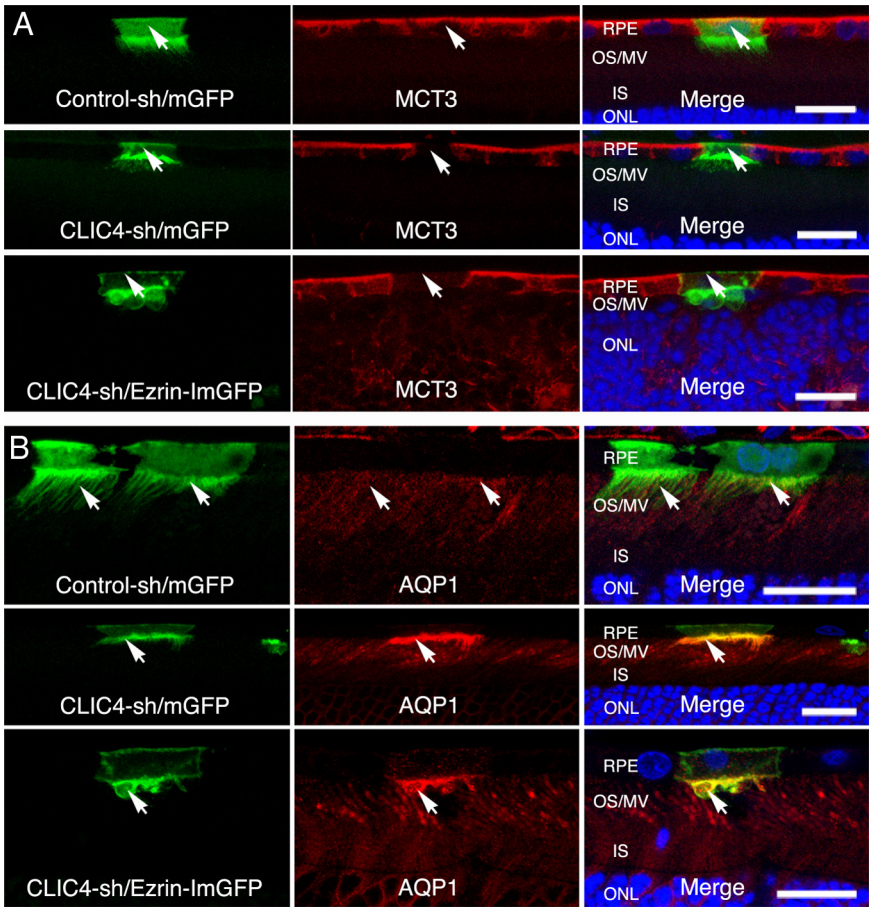

Figure 9. Altered MCT-3 and AQP1 expression patterns in CLIC4-suppressed RPE cells. Confocal images of retinal sections containing RPE cells transfected with the indicated plasmids and immunolabeled with MCT3 (A) or AQP1 (B). Arrows point to the transfected GFP^+ cells. Bars, 20 μm.

sults collectively suggested that CLIC4 attenuation induced specific changes in the expression patterns of transporters and channels in RPE cells.

DISCUSSION

In the present report, we showed that a member of CLIC proteins, CLIC4, was enriched at the apical RPE surfaces. Using a novel plasmid-based RPE-specific gene delivery method, we demonstrated that specific knockdown of CLIC4 in RPE cells in situ induces cytostructural remodeling of both RPE and neural retinas. Furthermore, CLIC4 attenuation in RPE cells weakens their adhesion to photoreceptor OS, thus producing a novel animal model of RD. Finally, we identified changes in the expression of transporter/channel triggered by CLIC4 suppression, delineating new targets for therapeutic intervention for RD.

Subcellular Distribution of CLIC4 in RPE Cells

Both biochemical and structural analyses suggested that CLIC4 is a globular cytosolic protein and is unlikely to behave as a typical pore-forming protein. However, purified, soluble recombinant CLIC4 was able to insert itself into artificial lipids and conduct a chloride ion current (Littler *et al.*, 2005). Furthermore, proteomics of surface-biotinylated inner medulla collecting duct proteins suggested that CLIC4 is an apical integral membrane protein in these cells (Yu *et al.*, 2006). The underlying mechanism for the membrane insertion of CLIC4 remains to be understood. Interestingly, recent studies showed that CLIC4 is structurally homologous to glutathione *S*-transferase and oxidation of CLIC4 enhances its binding to the lipid bilayer (Littler *et al.*, 2005; Singh and Ashley, 2007). In the present study, we showed that whereas cytoplasmic CLIC4 exists, it is highly enriched in the apical MV processes; our electron micrographs showed that CLIC4 is clearly in close apposition to the MV membranes, indicating that it is membrane associated. Future studies will be needed to investigate the topology of the membrane-bound CLIC4. Finally, because RPE is a tissue exposed to high levels of oxidative stress, we speculate that the elevated oxidative level increases the lipid membrane insertion of CLIC4.

Physiological Functions of CLIC4 in RPE Cells

The convoluted membranous folds of the apical MV and basal infoldings of RPE cells provide large surface areas attributable to their intimate interactions with neighboring cells and rapid exchange of ions, water, and metabolites. Our "reverse-genetics" analysis of RPE convincingly showed that lowering CLIC4 level is sufficient to disrupt both apical and basal membrane specialization even though the immunolabeling results suggested that it is predominant apical localization. It is possible that a trace amount of basal CLIC4 is functionally very potent. Alternatively, losing apical CLIC4 results in global effects on overall plasma membrane specialization, perhaps mediated through changes in the actin cytoskeleton and/or other yet-to-be discovered biosynthetic activities. It is worthy noting that both apical MV and basal infoldings are actin-enriched specialized membranes. Biochemical data has shown CLIC4 binds to

protein complexes containing actin and actin-binding proteins (Suginta *et al.,* 2001).

Knocking out ezrin also induces concomitant loss of both MV and basal infoldings in RPE cells even though ezrin, like CLIC4, is apically enriched (Bonilha *et al.,* 2006). Furthermore, the cytoplasmic inclusions containing MV-like membranes were similarly found in CLIC4-suppressed as well as ezrin-null RPE cells (Bonilha *et al.,* 2006). Ezrin is a well-characterized membrane-cytoskeleton linker (Tsukita and Yonemura, 1999; Bretscher *et al.,* 2002). It is concentrated in surface projections, such as MV or membrane ruffles, and is functionally involved in forming and/or stabilizing these specialized membranous structures (Bretscher *et al.,* 1997; Gautreau *et al.,* 2000). Previous studies showed that overexpressed ezrin increases the length of MV in RPE cultures in vitro (Bonilha *et al.,* 1999). Our results clearly show that forced expression of ezrin in RPE cells in situ produced excess apical membrane ruffle-like structures; ezrin overexpression induced ruffles was even more obvious in CLIC4-suppressed cells, raising an interesting possibility that CLIC4 influences ezrin-mediated MV morphogenesis. These results also strongly suggested that the functions of CLIC4 and ezrin in MV genesis are not redundant. Whether excess ezrin restores the basal infoldings of CLIC4-suppressed RPE is unclear and awaits future ultrastructural analysis.

It is important to note that except for the impaired MV, ezrin silencing fails to phenocopy other CLIC4-silencing induced abnormalities. For example, there was no altered expression of AQP1 (Supplemental Figure 4) or MCT3 (SD; Figure 3) in ezrin-sh–transfected RPE cells, nor detectable stress fibers, disrupted junctions (Supplemental Figure 5). Consistently, ezrin overexpression was unable to restore any of CLIC4-sh–mediated abnormalities (Figure 9). These results are consistent with the observation that no RD was reported for the ezrin-knockout mice (Bonilha *et al.,* 2006), supporting the idea that MV shortening per se cannot be accountable for the retinal detachment seen in CLIC4-suppressed RPE cells.

The pleiotropic effect caused by the attenuation of CLIC4 level suggests that it is likely that CLIC4 acts on a higher-order biosynthetic pathway for de novo membrane genesis. This process of membrane genesis is not only critical for the elongation of the RPE cell surface into MV or basal infoldings but also the overall cytoskeletal and junctional organization. Nevertheless, the morphological transformation of the RPE cells with CLIC4-suppressed resembles EMT, a process that is generally thought to be involved in the onset and progression of ocular proliferative disorders such as PVR.

RD Animal Model

Efficient net water movement in a subretina-to-choroid direction enables proper retinal attachment and function (Pederson, 1994). There are several sight-threatening eye diseases/injuries (e.g., macular edema, rhegmatogenous RD, and central serous chorioretinopathy) in which fluid accumulates within the retina or in the SRS. Although vitroretinal surgery has a high success rate in reattaching the retina anatomically, the functional recovery in patients is slow (up to several years; Kusaka *et al.,* 1998) and reoccurrence can take place even after successful reattachment. It would be highly desirable to find a less invasive drug treatment that can prevent RD or improve the outcome of reattachment surgery (e.g., stabilize the reattachment, reduce the damaging effects of detachment).

At present, the molecular basis underlying the physical separation between the RPE and retina is poorly understood, underscoring the value of animal models of RD. A widely used RD animal model can be achieved by subretinal delivery of a small volume of reagents (e.g., saline, sodium hyaluronate; Guerin *et al.,* 1990; Rattner and Nathans, 2005; Farjo *et al.,* 2008). Many manifestations seen in the RPE and retina of this type of RD model were detected in our CLIC4-shRNA rat model. In our animals, the site of detachment is restricted to the area immediately near the targeted RPE cells, whereas the injury of neural retinas appears to be widespread, indicating that the "signal" stemming from the dystrophied RPE is diffusible and propagated in the neural retina. In addition to GFAP being activated in the Muller cells, the expression levels and patterns of several other molecules (e.g., NKCC1, Na/K-ATPase) were also drastically altered in these retinas (unpublished results); such changes could also be attributed to the deformation of the neural retinas.

Of great interest, we identified profound changes in the expression patterns of MCT3 and AQP1 in CLIC4-suppressed RPE cells. Both the disappearance of basal MCT3 and appearance of apical AQP1 were discrete and can be consistently detected by immunohistochemical labeling. Furthermore, these changes can be readily detected in RPE cells that still had a relatively normal morphological appearance, indicating that these are early changes and are likely to be causally linked to the SRS fluid accumulation and RD. MCT3 is the basal counterpart of apical MCT1, which has a confirmed role in cotransport of H^+, lactate, and water in RPE cells (Hamann *et al.,* 2003). Loss of MCT3 may reduce the efficiency of the net SRS-to-choroid water transport. AQP, on the hand, is a constitutive channel for water (Agre *et al.,* 1993). AQP in the ocular system is thought to be more important for fluid accumulation (vs. fluid depletion; Nielsen *et al.,* 1993; Oshio *et al.,* 2005). Therefore, the upregulation of AQP1 that appeared in the apical surfaces of CLIC4-suppressed cells could directly contribute to the subretinal fluid accumulation. Nevertheless, recent studies showed that in vitro–cultured RPE cells overexpressing AQP1 had increased water movement across cells (Stamer *et al.,* 2003), posing the possibility that AQP1 may act in pumping water as part of functional compensation. Although further investigation is needed to distinguish these two possibilities, we propose that these molecules are excellent candidate targets for RD therapy.

RPE cells with CLIC4 knockdown also had impaired TJ structures. The TJ of RPE cells is a critical part of the blood-retina barrier and increased permeability of RPE has been associated with animal models of diabetes as well as RD-related conditions (Cunha-Vaz, 1976; Bresnick, 1986). The increased paracellular fluid transport caused by TJ leakage could also, in part, contribute to the SRS fluid accumulation in RD.

We do not know the mechanism by which the level of CLIC4 influences the expression patterns of proteins such as AQP1 and MCT3 in RPE cells. However, CLIC4 has been reported to act as a transcriptional cofactor in keratinocytes (Yao *et al.,* 2009). Furthermore, several junctional components are directly linked to signaling and transcriptional pathways (Kim *et al.,* 2008; Balda and Matter, 2009). It is possible that the TJ structural impairment of CLIC4-suppressed cells is causally associated with the transcriptional regulation of AQP1 and/or MCT3.

Efficient and Versatile Approach to Modulating Gene Expression in RPE in Vivo

There is currently no coculture system available that mimics the tightly associated photoreceptor-RPE-choroid tissue. Although virus-based subretinal injection is an effective means

to conduct RPE gene delivery, virus preparation is nevertheless time-consuming and labor intensive. Although reporter plasmids have been successful delivered into RPE of adult animals for promoter analysis (Kachi *et al.*, 2006; Esumi *et al.*, 2009), we here showed the plasmid-based transfection procedure provides a versatile, rapid, safe, cost-effective approach to perform both gain- and loss-of-function analysis and to study the cell biology of RPE cells in situ. The use of a reporter allows the unambiguous identification of the targeted cells and allows the study of their cell-autonomous effect(s) in the context of neighboring control cells, at both light microscopic and ultrastructural levels. Furthermore, phenotypes seen in the transfected RPE cells reproduce the results of previous transgenic mouse studies (e.g., ezrin knockout mice; Bonilha *et al.*, 2006). Nevertheless, concerns about differences in genetic background encountered in transgenic mouse studies are largely avoided in this approach. Finally, future incorporation of an inducible knockdown or expression plasmid would further advance the usefulness of this model system, and certainly it will be an invaluable tool to model diseased RPE and to complement the RPE-specific transgenic mouse approach.

ACKNOWLEDGMENTS

We thank Drs. Daniel Stamer, Monique Arpin, Nancy Philp, Yang Shi, Robert Molday, Jim Turner, and Connie Cepko for reagents and Joseph Wang for the drawing in Figure 1A. We also thank Drs. Mark Berryman, Janet Sparrow, Enrique Rodgriguez-Boulan, and Siliva Finnemann for useful discussions during the course of this study. This work was supported by Research To Prevent Blindness, The Irma T. Hirsch Trust, The Ruth and Milton Steinbach Fund, and National Institutes of Health Grants EY016805 and EY11307.

REFERENCES

Agre, P., Preston, G. M., Smith, B. L., Jung, J. S., Raina, S., Moon, C., Guggino, W. B., and Nielsen, S. (1993). Aquaporin CHIP: the archetypal molecular water channel. Am. J. Physiol. *265*, F463–F476.

Algrain, M., Turunen, O., Vaheri, A., Louvard, D., and Arpin, M. (1993). Ezrin contains cytoskeleton and membrane binding domains accounting for its proposed role as a membrane-cytoskeletal linker. J. Cell Biol. *120*, 129–139.

Ashley, R. H. (2003). Challenging accepted ion channel biology: p64 and the CLIC family of putative intracellular anion channel proteins [Review]. Mol. Membr. Biol. *20*, 1–11.

Balda, M. S., and Matter, K. (2009). Tight junctions and the regulation of gene expression. Biochim. Biophys. Acta *1788*, 761–767.

Berry, K. L., Bulow, H. E., Hall, D. H., and Hobert, O. (2003). A *C. elegans* CLIC-like protein required for intracellular tube formation and maintenance. Science *302*, 2134–2137.

Berryman, M., and Bretscher, A. (2000). Identification of a novel member of the chloride intracellular channel gene family (CLIC5) that associates with the actin cytoskeleton of placental microvilli. Mol. Biol. Cell *11*, 1509–1521.

Berryman, M. A., and Goldenring, J. R. (2003). CLIC4 is enriched at cell-cell junctions and colocalizes with AKAP350 at the centrosome and midbody of cultured mammalian cells. Cell Motil. Cytoskelet. *56*, 159–172.

Bohman, S., Matsumoto, T., Suh, K., Dimberg, A., Jakobsson, L., Yuspa, S., and Claesson-Welsh, L. (2005). Proteomic analysis of vascular endothelial growth factor-induced endothelial cell differentiation reveals a role for chloride intracellular channel 4 (CLIC4) in tubular morphogenesis. J. Biol. Chem. *280*, 42397–42404.

Bonilha, V. L., Finnemann, S. C., and Rodriguez-Boulan, E. (1999). Ezrin promotes morphogenesis of apical microvilli and basal infoldings in retinal pigment epithelium. J. Cell Biol. *147*, 1533–1548.

Bonilha, V. L., Rayborn, M. E., Saotome, I., McClatchey, A. I., and Hollyfield, J. G. (2006). Microvilli defects in retinas of ezrin knockout mice. Exp. Eye Res. *82*, 720–729.

Bresnick, G. H. (1986). Diabetic macular edema. A review. Ophthalmology *93*, 989–997.

Bretscher, A. (1989). Rapid phosphorylation and reorganization of ezrin and spectrin accompany morphological changes induced in A-431 cells by epidermal growth factor. J. Cell Biol. *108*, 921–930.

Bretscher, A., Edwards, K., and Fehon, R. G. (2002). ERM proteins and merlin: integrators at the cell cortex. Nat. Rev. Mol. Cell Biol. *3*, 586–599.

Bretscher, A., Reczek, D., and Berryman, M. (1997). Ezrin: a protein requiring conformational activation to link microfilaments to the plasma membrane in the assembly of cell surface structures. J. Cell Sci. *110*(Pt 24), 3011–3018.

Bringmann, A., and Reichenbach, A. (2001). Role of Muller cells in retinal degenerations. Front Biosci. *6*, E72–E92.

Chan, J., Aoki, C., and Pickel, V. M. (1990). Optimization of differential immunogold-silver and peroxidase labeling with maintenance of ultrastructure in brain sections before plastic embedding. J. Neurosci. Methods *33*, 113–127.

Chen, L., Wu, W., Dentchev, T., Zeng, Y., Wang, J., Tsui, I., Tobias, J. W., Bennett, J., Baldwin, D., and Dunaief, J. L. (2004). Light damage induced changes in mouse retinal gene expression. Exp. Eye Res. *79*, 239–247.

Chuang, J. Z., Milner, T. A., and Sung, C. H. (2001). Subunit heterogeneity of cytoplasmic dynein: differential expression of 14 kDa dynein light chains in rat hippocampus. J. Neurosci. *21*, 5501–5512.

Chuang, J. Z., Milner, T. A., Zhu, M., and Sung, C. H. (1999). A 29 kDa intracellular chloride channel p64H1 is associated with large dense-core vesicles in rat hippocampal neurons. J. Neurosci. *19*, 2919–2928.

Cunha-Vaz, J. G. (1976). The blood-retinal barriers. Doc. Ophthalmol. *41*, 287–327.

Duncan, R. R., Westwood, P. K., Boyd, A., and Ashley, R. H. (1997). Rat brain p64H1, expression of a new memer of the p64 chloride channel protein family in endoplasmic reticulum. J. Biol. Chem. *272*, 23880–23886.

Dunn, K. C., Aotaki-Keen, A. E., Putkey, F. R., and Hjelmeland, L. M. (1996). ARPE-19, a human retinal pigment epithelial cell line with differentiated properties. Exp. Eye Res. *62*, 155–169.

Edelman, J. L., and Miller, S. S. (1991). Epinephrine stimulates fluid absorption across bovine retinal pigment epithelium. Invest. Ophthalmol. Vis. Sci. *32*, 3033–3040.

Edwards, J. C. (1999). A novel p64-related Cl-channel: subcellular distribution and nephron segment-specific expression. Am. J. Physiol. *276*, F398–F408.

Esumi, N., Kachi, S., Hackler, L., Jr., Masuda, T., Yang, Z., Campochiaro, P. A., and Zack, D. J. (2009). BEST1 expression in the retinal pigment epithelium is modulated by OTX family members. Hum. Mol. Genet. *18*, 128–141.

Farjo, R., Peterson, W. M., and Naash, M. I. (2008). Expression profiling after retinal detachment and reattachment: a possible role for aquaporin-0. Invest. Ophthalmol. Vis. Sci. *49*, 511–521.

Fernandez-Salas, E., *et al.* (2002). mtCLIC/CLIC4, an organellular chloride channel protein, is increased by DNA damage and participates in the apoptotic response to p53. Mol. Cell. Biol. *22*, 3610–3620.

Finnemann, S. C., Bonilha, V. L., Marmorstein, A. D., and Rodriguez-Boulan, E. (1997). Phagocytosis of rod outer segments by retinal pigment epithelial cells requires alpha(v)beta5 integrin for binding but not for internalization. Proc. Natl. Acad. Sci. USA *94*, 12932–12937.

Fisher, S. K., Lewis, G. P., Linberg, K. A., and Verardo, M. R. (2005). Cellular remodeling in mammalian retina: results from studies of experimental retinal detachment. Prog. Retin Eye Res. *24*, 395–431.

Gautreau, A., Louvard, D., and Arpin, M. (2000). Morphogenic effects of ezrin require a phosphorylation-induced transition from oligomers to monomers at the plasma membrane. J. Cell Biol. *150*, 193–203.

Guerin, C. J., Anderson, D. H., and Fisher, S. K. (1990). Changes in intermediate filament immunolabeling occur in response to retinal detachment and reattachment in primates. Invest. Ophthalmol. Vis. Sci. *31*, 1474–1482.

Gundersen, D., Orlowski, J., and Rodriguez-Boulan, E. (1991). Apical polarity of Na,K-ATPase in retinal pigment epithelium is linked to a reversal of the ankyrin-fodrin submembrane cytoskeleton. J. Cell Biol. *112*, 863–872.

Hamann, S., Kiilgaard, J. F., la Cour, M., Prause, J. U., and Zeuthen, T. (2003). Cotransport of H^+, lactate, and H2O in porcine retinal pigment epithelial cells. Exp. Eye Res. *76*, 493–504.

Hamann, S., Zeuthen, T., La Cour, M., Nagelhus, E. A., Ottersen, O. P., Agre, P., and Nielsen, S. (1998). Aquaporins in complex tissues: distribution of aquaporins 1–5 in human and rat eye. Am. J. Physiol. *274*, C1332–C1345.

Iandiev, I., Pannicke, T., Reichel, M. B., Wiedemann, P., Reichenbach, A., and Bringmann, A. (2005). Expression of aquaporin-1 immunoreactivity by photoreceptor cells in the mouse retina. Neurosci. Lett. *388*, 96–99.

Kachi, S., Esumi, N., Zack, D. J., and Campochiaro, P. A. (2006). Sustained expression after nonviral ocular gene transfer using mammalian promoters. Gene Ther. *13*, 798–804.

Kim, J. W., Kang, K. H., Burrola, P., Mak, T. W., and Lemke, G. (2008). Retinal degeneration triggered by inactivation of PTEN in the retinal pigment epithelium. Genes Dev. *22*, 3147–3157.

Kusaka, S., Toshino, A., Ohashi, Y., and Sakaue, E. (1998). Long-term visual recovery after scleral buckling for macula-off retinal detachments. Jpn. J. Ophthalmol. *42*, 218–222.

Littler, D. R., *et al*. (2005). Crystal structure of the soluble form of the redox-regulated chloride ion channel protein CLIC4. FEBS J. *272*, 4996–5007.

Lubarsky, B., and Krasnow, M. A. (2003). Tube morphogenesis: making and shaping biological tubes. Cell *112*, 19–28.

Matsuda, T., and Cepko, C. L. (2004). Inaugural Article: Electroporation and RNA interference in the rodent retina in vivo and in vitro. Proc. Natl. Acad. Sci. USA *101*, 16–22.

Moore-Hoon, M. L., and Turner, R. J. (1998). Molecular and topological characterization of the rat parotid Na^+-K^+-$2Cl^-$ cotransporter1. Biochim. Biophys. Acta *1373*, 261–269.

Nabi, I. R., Mathews, A. P., Cohen-Gould, L., Gundersen, D., and Rodriguez-Boulan, E. (1993). Immortalization of polarized rat retinal pigment epithelium. J. Cell Sci. *104*(Pt 1), 37–49.

Nielsen, S., Smith, B. L., Christensen, E. I., and Agre, P. (1993). Distribution of the aquaporin CHIP in secretory and resorptive epithelia and capillary endothelia. Proc. Natl. Acad. Sci. USA *90*, 7275–7279.

Oshio, K., Watanabe, H., Song, Y., Verkman, A. S., and Manley, G. T. (2005). Reduced cerebrospinal fluid production and intracranial pressure in mice lacking choroid plexus water channel Aquaporin-1. FASEB J. *19*, 76–78.

Pederson, J. (1994). Fluid physiology of the subretinal space. In: Retina, ed. C. E. Wilkinson, St. Louis: Mosby.

Philp, N. J., Wang, D., Yoon, H., and Hjelmeland, L. M. (2003). Polarized expression of monocarboxylate transporters in human retinal pigment epithelium and ARPE-19 cells. Invest. Ophthalmol. Vis. Sci. *44*, 1716–1721.

Philp, N. J., Yoon, H., and Grollman, E. F. (1998). Monocarboxylate transporter MCT1 is located in the apical membrane and MCT3 in the basal membrane of rat RPE. Am. J. Physiol. *274*, R1824–R1828.

Rattner, A., and Nathans, J. (2005). The genomic response to retinal disease and injury: evidence for endothelin signaling from photoreceptors to glia. J. Neurosci. *25*, 4540–4549.

Rattner, A., Toulabi, L., Williams, J., Yu, H., and Nathans, J. (2008). The genomic response of the retinal pigment epithelium to light damage and retinal detachment. J. Neurosci. *28*, 9880–9889.

Ruiz, A., and Bok, D. (1996). Characterization of the 3′ UTR sequence encoded by the AQP-1 gene in human retinal pigment epithelium. Biochim. Biophys. Acta *1282*, 174–178.

Sethi, C. S., Lewis, G. P., Fisher, S. K., Leitner, W. P., Mann, D. L., Luthert, P. J., and Charteris, D. G. (2005). Glial remodeling and neural plasticity in human retinal detachment with proliferative vitreoretinopathy. Invest. Ophthalmol. Vis. Sci. *46*, 329–342.

Shukla, A., Malik, M., Cataisson, C., Ho, Y., Friesen, T., Suh, K. S., and Yuspa, S. H. (2009). TGF-beta signalling is regulated by Schnurri-2-dependent nuclear translocation of CLIC4 and consequent stabilization of phospho-Smad2 and 3. Nat. Cell Biol. *11*, 777–784.

Singh, H., and Ashley, R. H. (2007). CLIC4 (p64H1) and its putative transmembrane domain form poorly selective, redox-regulated ion channels. Mol. Membr. Biol. *24*, 41–52.

Stamer, W. D., Bok, D., Hu, J., Jaffe, G. J., and McKay, B. S. (2003). Aquaporin-1 channels in human retinal pigment epithelium: role in transepithelial water movement. Invest. Ophthalmol. Vis. Sci. *44*, 2803–2808.

Steinberg, R. H. (1986). Research update: report from a workshop on cell biology of retinal detachment. Exp. Eye Res. *43*, 695–706.

Suginta, W., Karoulias, N., Aitken, A., and Ashley, R. H. (2001). Chloride intracellular channel protein CLIC4 (p64H1) binds directly to brain dynamin I in a complex containing actin, tubulin and 14-3-3 isoforms. Biochem. J. *359*, 55–64.

Suh, K. S., *et al*. (2004). The organellular chloride channel protein CLIC4/mtCLIC translocates to the nucleus in response to cellular stress and accelerates apoptosis. J. Biol. Chem. *279*, 4632–4641.

Tsukita, S., and Yonemura, S. (1999). Cortical actin organization: lessons from ERM (ezrin/radixin/moesin) proteins. J. Biol. Chem. *274*, 34507–34510.

Verkman, A. S., Ruiz-Ederra, J., and Levin, M. H. (2008). Functions of aquaporins in the eye. Prog. Retin. Eye Res. *27*, 420–433.

Xia, X. G., Zhou, H., Ding, H., el Affar, B., Shi, Y., and Xu, Z. (2003). An enhanced U6 promoter for synthesis of short hairpin RNA. Nucleic Acids Res. *31*, e100.

Yao, Q., Qu, X., Yang, Q., Wei, M., and Kong, B. (2009). CLIC4 mediates TGF-beta1-induced fibroblast-to-myofibroblast transdifferentiation in ovarian cancer. Oncol. Rep. *22*, 541–548.

Yonemura, S., and Tsukita, S. (1999). Direct involvement of ezrin/radixin/moesin (ERM)-binding membrane proteins in the organization of microvilli in collaboration with activated ERM proteins. J. Cell Biol. *145*, 1497–1509.

Yu, M. J., Pisitkun, T., Wang, G., Shen, R. F., and Knepper, M. A. (2006). LC-MS/MS analysis of apical and basolateral plasma membranes of rat renal collecting duct cells. Mol. Cell Proteom. *5*, 2131–2145.

Zacks, D. N., Han, Y., Zeng, Y., and Swaroop, A. (2006). Activation of signaling pathways and stress-response genes in an experimental model of retinal detachment. Invest. Ophthalmol. Vis. Sci. *47*, 1691–1695.

Zhao, S., Rizzolo, L. J., and Barnstable, C. J. (1997). Differentiation and transdifferentiation of the retinal pigment epithelium. Int. Rev. Cytol. *171*, 225–266.